

# Transmission Line Fault Classification Based on Higher-Order Spectrum and ResNet

Zhenjie Wang<sup>1</sup> & Shanhua Yao<sup>1</sup>

<sup>1</sup> School of Electrical and Information Engineering, Anhui University of Science and Technology, Anhui, China  
Correspondence: Zhenjie Wang, School of Electrical and Information Engineering, Anhui University of Science and Technology, Anhui, China.

doi:10.56397/IST.2023.07.07

## Abstract

The accurate classification of transmission line faults has been a key issue in the development of smart grids. At present, fault classification is based on recurrent neural network (RNN) for temporal signals, and the development of RNN is not so mature compared with convolutional neural network (CNN). Therefore, this paper proposes a transmission line fault classification algorithm based on higher-order spectral analysis and CNN, aiming at converting the time-series signals into images and using CNN for fault classification. After establishing the fault model on Matlab/Simulink, the current signals of different faults are obtained. After processing the current signals to extract their zero-mode currents, the fault image signals are obtained using higher-order spectral analysis as the input to the CNN. Simulation results show that the proposed method can accurately identify faults with high accuracy when faults occur in transmission lines, thus reducing the economic losses caused by faults.

**Keywords:** transmission lines, higher-order spectrum, convolutional neural network (CNN), smart grids

## 1. Introduction

The power system has five main links: power generation, power transformation, power transmission, power distribution and power consumption, of which transmission and distribution are the intermediate links and play the function of transmission. Each link is composed of generators, transformers, transmission lines, distribution lines and other devices. The transmission line is an important facility for transmitting electric power in the power system. In the power system, short-circuit faults can cause huge losses if the zone protection of each part is not installed with corresponding relay protectors. Among these, transmission line faults account for about 50% of the total faults (J. Rajashekar & A. Yadav, 2022). The probability of single-phase grounding fault is the largest, accounting for about 80% of the total number of faults in the distribution network, while single-phase grounding faults, when not repaired in time, can then evolve into phase-to-phase ground faults.

With the innovation in recent years, the traditional power system has developed to a smart grid power system, the traditional model-based technology is more difficult to carry out on the more open and complex smart grid, artificial intelligence is the key to the future progress and development of smart grid. The increasing complexity and variability of the distribution grid operating environment as well as the continuous development of a large scale, the probability of failure is relatively high. Grounding faults will not only lead to serious safety problems, but also adversely affect the power supply quality of the power system.

At present, researchers at home and abroad have achieved some results in fault diagnosis of transmission lines. The literature (Li LF, Rao D, Fan R, Zhang H, Wang J, Luo HY, Liu Z & Xu GH, 2022) takes the pre-processed traveling wave data and trains the data using Long-Short term Memory (LSTM) networks. In the literature (Liu F, Li YK, Gao F, et al, 2021), wavelet scattering feature extraction is performed on the fault zero sequence current signal to obtain the fault feature vector, which is then input to the Bi-LSTM network for training. The literature

(R. Resmi, V. Vanitha, E. Aravind, B. R. Sundaram, C. R. Aswin & S. Harithaa, 2019) provides all the collected three-phase voltages and currents to the Artificial Neural Network (ANN) algorithm for detecting the fault type. The literature (M. R. Bishal, S. Ahmed, N. M. Molla, K. M. Mamun, A. Rahman & M. A. A. Hysam, 2021) developed artificial neural network algorithm using feedforward artificial neural network. The root means square values of the collected three-phase voltages and currents are fed into the ANN for fault classification. In the literature (M. Li, Y. Yu, T. Ji & Q. Wu, 2019), in order to improve the training speed of traditional LSTM networks, FC-LSTM networks were proposed to reduce the training complexity of the temporal data by adding a filter to enhance the calibration. In the literature (Z. Wan, L. Hui & L. Yongkang, 2020), the zero-sequence current after a fault is decomposed into variable modes, and the decomposed signal and the original signal are input to a Bi-LSTM network for fault diagnosis.

However, current transmission line fault diagnosis is performed by researchers using temporal data and using RNN for fault detection and classification. The technical aspects of temporal data processing may not be as mature as image processing compared to image processing. However, in terms of image processing, transmission line fault diagnosis mostly refers to unmanned aircraft inspection and the diagnosis of external faults such as insulator defects (Y. Bao & T. Chen, 2020; X. Liu, X. Miao, H. Jiang & J. Chen, 2021; X. Zhang et al, 2021).

In this paper, a new fault diagnosis algorithm will be proposed to convert the collected temporal data into image data, i.e., temporal processing into image processing. The technology of neural network in image processing is very mature, and better fault diagnosis results can be obtained by using image processing.

**2. High-Order Spectral Analysis**

Higher-order spectral analysis is a method that allows an efficient feature extraction of the signal and usually requires the calculation of the bispectrum and the bicoherence spectrum, which is the normalized bispectrum (L. Gagliano, E. B. Assi, M. Sawan & D. K. Nguyen, 2018). This method is based on the Fourier transform of the higher-order correlation function, which provides information on phase and power and allows the detection of asymmetric nonlinearities between different frequency components of the signal.

Higher-order spectral analysis is very effective in identifying nonlinear and non-Gaussian stochastic processes and deterministic signals, and among them, second-order spectral analysis (Yu F, Zhao J, Qiu Z. Y et al, 2022) is widely used in fields such as image reconstruction. The second-order spectral analysis method can well suppress the phase relations in the signal and detect and quantify the phase coupling of non-Gaussian signals. In this paper, this method is applied to the feature extraction of faulty fault signals.

The bispectrum is a complex quantity and the equation can be expressed as:

$$\begin{aligned}
 & Bis_x(f_1, f_2) \\
 &= \sum_{\tau_1=-\infty}^{+\infty} \sum_{\tau_2=-\infty}^{+\infty} c_3^x(\tau_1, \tau_2) e^{-j2\pi(f_1\tau_1+f_2\tau_2)}
 \end{aligned} \tag{1}$$

$$c_3^x(\tau_1, \tau_2) = E(x(n)x(n+\tau_1)x(n+\tau_2)) \tag{2}$$

Where  $f_1, f_2$  are two frequency variables,  $\tau_1, \tau_2$  are time lag constants,  $Bis_x(f_1, f_2)$  is the bispectrum, and  $c_3^x(\tau_1, \tau_2)$  is the third order cumulative quantity, E is the arithmetic average.

Normalization of the bispectrum, which is calculated by dividing the bispectrum by the square root of the actual triple product of the power spectrum, provides a quantitative indicator of the variance independent of the signal energy and is referred to as the bicoherent spectrum, as shown in:

$$\begin{aligned}
 & Bic^2(f_1, f_2) = \\
 & \frac{|Bis_x(f_1, f_2)|^2}{\frac{1}{K} \sum_{i=0}^{K-1} |X_i(f_1)X_i(f_2)|^2 \frac{1}{K} \sum_{i=0}^{K-1} |X_i(f_1+f_2)|^2}
 \end{aligned} \tag{3}$$

where  $X(f)$  denotes the Fourier transform value of  $X(f)$  at frequency  $f$ .

**3. Convolutional Neural Networks**

The deeper the depth of the convolutional network, the more advanced the extracted features and the better the performance, but the traditional CNN faces the problems of network degradation, gradient disappearance and gradient explosion as the depth of layers increases, making the performance of the higher-level network instead inferior to that of the shallow network. Therefore, this paper draws on the classical CNN model ResNet50.

The design idea of ResNet50 is to solve the problem of gradient disappearance and model degradation in deep networks through residual connectivity, thus ensuring that the model can better learn feature representations. The residual module is shown in Figure 1, where  $x$  is the constant mapping and  $F(x)$  is the residual mapping. The input,  $x$ , is divided into two ways, with the input  $x$  entering the first weight layer to obtain the mapping function  $F(x)$ ; the Relu activation function is used to enter the second weight layer. The two are summed into the activation function and then the output  $\text{Relu}(F(x)+x)$ . The residual network enhances the exchange of information and communication between network layers by connecting across layers and mapping shallow features directly into deep features.

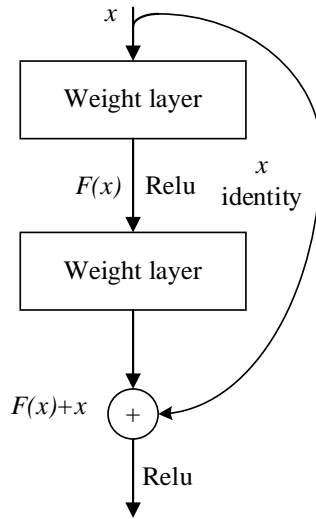


Figure 1. Residuals module

ResNet50 is a deep convolutional neural network architecture for image classification, with 50 layers. The input image is typically 224 x 224 pixels with 3 channels (RGB). The ResNet50 architecture consists of five convolutional stages, each consisting of residual blocks and shortcut connections. The final fully connected layer and Softmax activation are responsible for mapping features into classification probabilities, and the main structure is shown in Table 1.

Table 1. Resnet50 main structure

Layer name	Output size	ResNet50
Conv1	112×112	7×7, 64, stride 2 3×3 max pool, stride 2
Conv2_x	56×56	$\begin{bmatrix} 1 \times 1, 64 \\ 3 \times 3, 64 \\ 1 \times 1, 256 \end{bmatrix} \times 3$
Conv3_x	28×28	$\begin{bmatrix} 1 \times 1, 128 \\ 3 \times 3, 128 \\ 1 \times 1, 512 \end{bmatrix} \times 4$
Conv4_x	14×14	$\begin{bmatrix} 1 \times 1, 256 \\ 3 \times 3, 256 \\ 1 \times 1, 1024 \end{bmatrix} \times 6$
Conv5_x	7×7	$\begin{bmatrix} 1 \times 1, 512 \\ 3 \times 3, 512 \\ 1 \times 1, 2048 \end{bmatrix} \times 3$
Flops	1×1	Average pool, 1000d-d fc, softmax 3.8×10 <sup>9</sup>

### 4. Simulation Results

In order to verify the performance of the proposed algorithm, the transmission line model shown in Figure 2 is built in Matlab/Simulink.

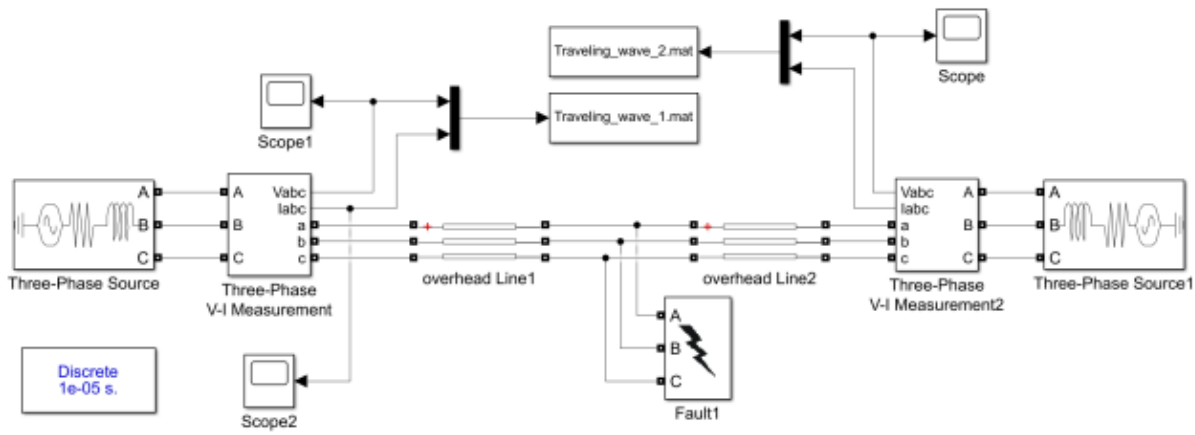


Figure 2. Schematic diagram of transmission line model

In Figure 2, a transmission line fault model with a total length of 200 km, 220 kV, and 50 Hz is constructed. The model is connected to the power supply at both ends, and the fault current signal at one end is measured by a measurement element with a sampling rate of 100 KHZ. The acquired fault current signal is phase-mode transformed to obtain its zero-mode component, which provides the necessary data for transmission line fault diagnosis. The next step uses second-order spectral analysis to transform the processed current signal into a two-bit feature image, which preserves as much as possible the useful features of the signal. The specific parameters are shown in Table 2.

Table 2. Experimental parameters

Failure parameters	Fault Type	AG,BG,CG,AB,BC,CA,ABG,BCG,CAG,ABC
	Fault distance (Km)	5,6,7,8,...,195
	Fault resistance ( $\Omega$ )	0.01,1,10,50,100
Transmission line parameters	Positive sequence and zero sequence resistance ( $\Omega$ /Km)	0.17,0.23
	Positive sequence and zero sequence inductance (H/Km)	1.21e-3,5.48e-3
	Positive sequence and zero sequence capacitance (F/Km)	9.7e-9,6e-9
Power supply parameters	Phase voltage (V)	220k
	Frequency	50Hz

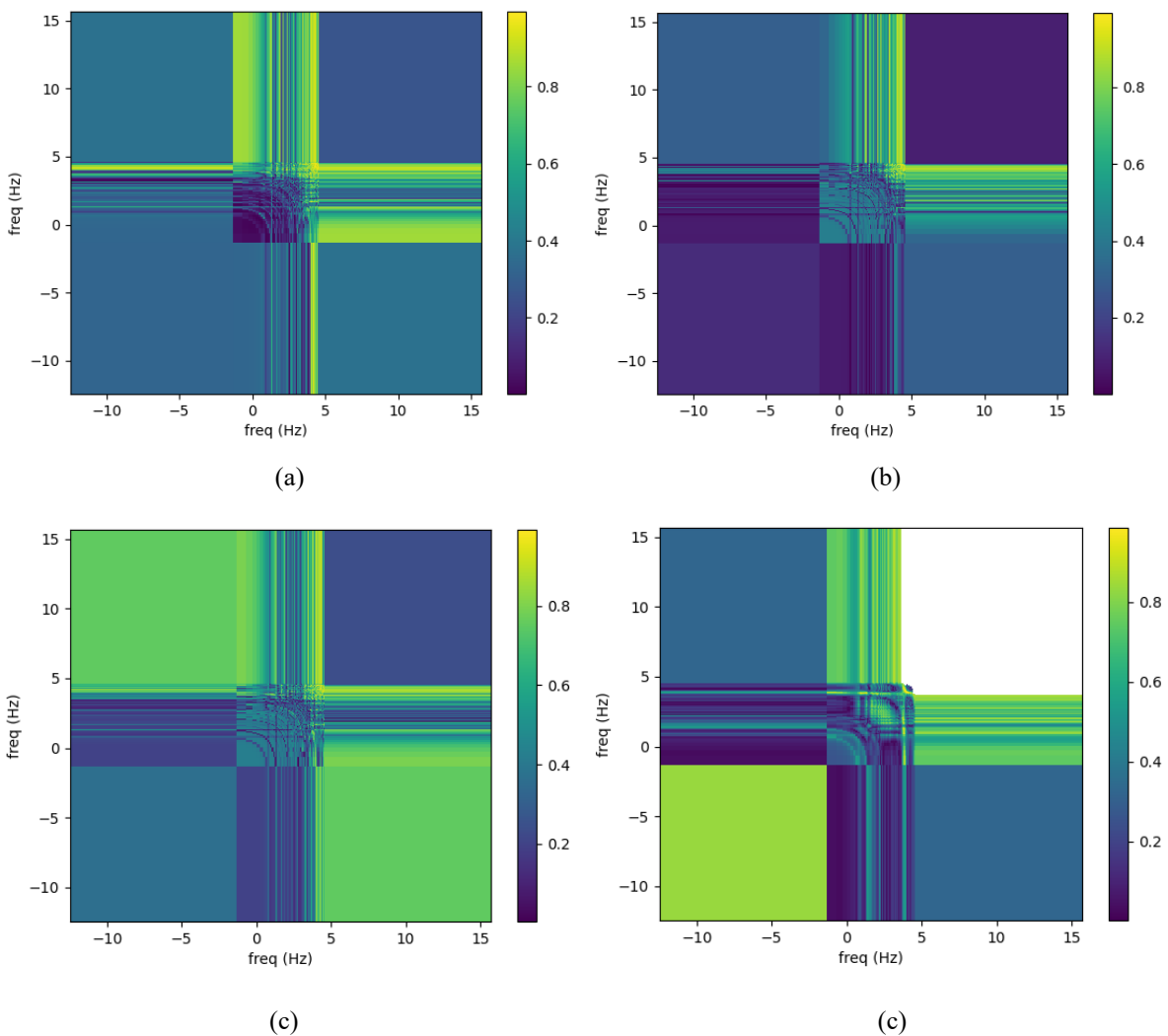
Simulate all the fault cases in Matlab/Simulink and perform phase mode transformation on the fault current signals to get all the zero sequence current signals. Export all the zero sequence current signals as mat files for saving to prevent data loss. For the stored zero sequence current signals, the second order spectral features are extracted in turn, and each zero sequence current timing signal is transformed into a two-dimensional feature image of the zero sequence current, as shown in Figure 3.

Figure 3 shows the fault images extracted by second-order spectral analysis. Due to the large number of fault images, only images of each fault type were randomly selected from the various types of faults. These fault images were labelled to reflect each of the ten fault types as shown in Table 3. After second-order spectrum extraction, although all images of the same fault were slightly different, their key features could be accurately discriminated by the neural network.

Table 3. Fault types and corresponding labels

Fault Type	Label
AG	1
BG	2
CG	3
AB	4
BC	5
CA	6
ABG	7
BCG	8
CAG	9
ABC	10

In this aspect of image classification, CNN is the most maturely developed, and this time ResNet50 will be used to perform fault diagnosis. In this paper, 9550 fault sample sets are obtained by Matlab/Simulink simulation for ten types of faults and five different fault resistances. The sample set is divided into training set, validation set and test set according to the ratio of 8:1:1. The neural network learning rate was set to 0.001, the batch size was set to 128, the number of iteration rounds was 13, and the optimizer was selected as adam optimizer. Figure 4 shows the accuracy and loss of the training, where the accuracy of the validation set is 99.06% and the accuracy of the test set is 99.26%.



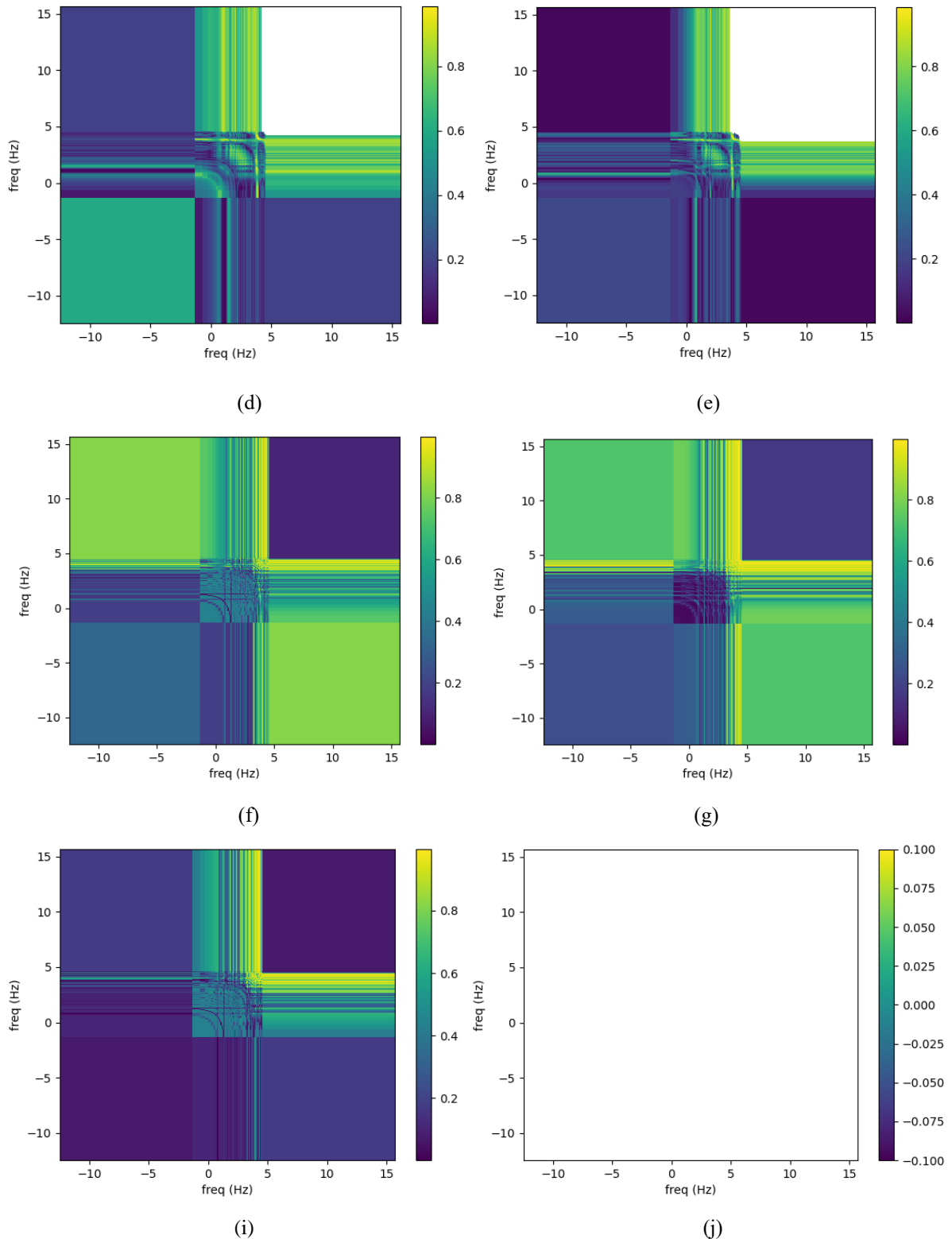


Figure 3. Second-order spectrum of fault signal

Note: (a) Second-order spectrum of AG faults; (b) Second-order spectrum of BG faults; (c) Second-order spectrum of CG faults; (d) Second-order spectrum of AB faults; (e) Second-order spectrum of BC faults; (f) Second-order spectrum of CA faults; (g) Second-order spectrum of ABG faults; (h) Second-order spectrum of BCG faults; (i) Second-order spectrum of CAG faults; (j) Second-order spectrum of ABC faults

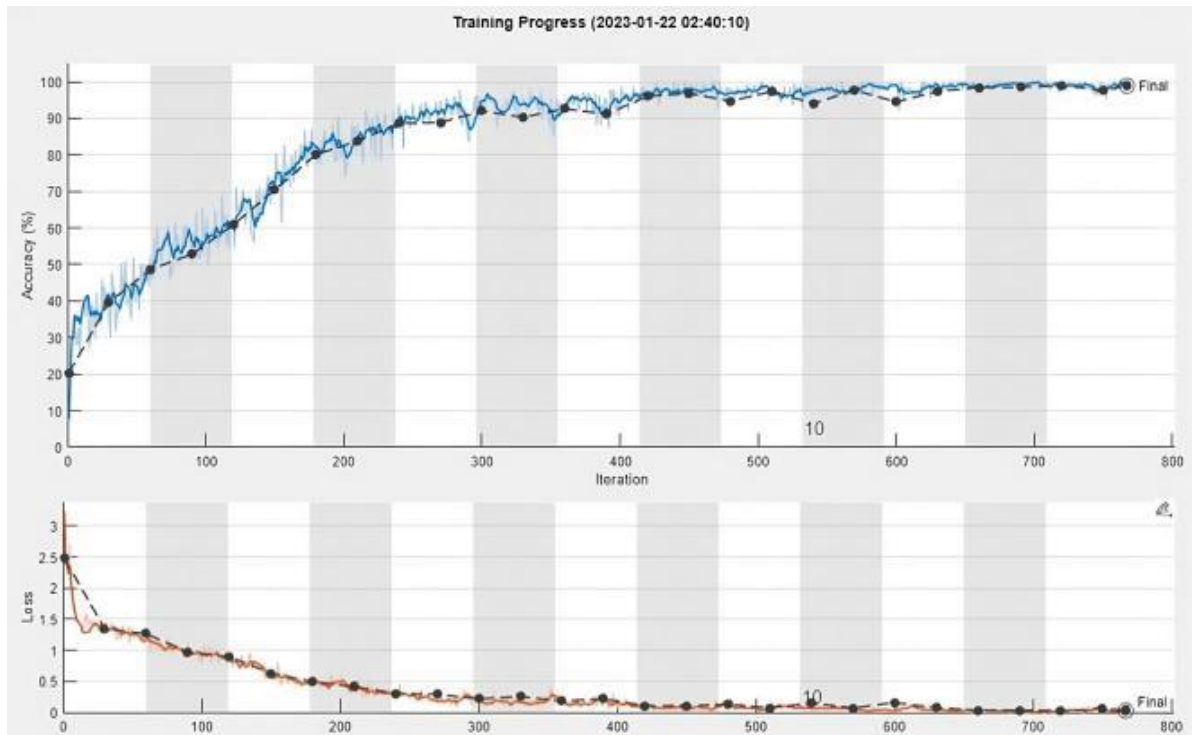


Figure 4. Training progress chart

In order to comparatively assess the superiority of the performance of the proposed method in this paper, an objective evaluation of each type of algorithm is performed, and the results are shown in Table 4.

Table 4. Comparison of algorithms

Algorithms	Accuracy
Algorithm in this paper	99.26%
Algorithm in literature (J. Rajashekar & A. Yadav, (2022)	96.7%
Algorithm in literature (A. Bhuyan, B. K. Panigrahi, K. Pal & S. Pati, 2022)	95.45%

The algorithm proposed in the literature (J. Rajashekar & A. Yadav, 2022) feeds fault and unfaulted current and voltage data into an LSTM network and achieves an accuracy of 96.7% for its test set. The algorithm proposed in (A. Bhuyan, B. K. Panigrahi, K. Pal & S. Pati, 2022) feeds all fault current and time maps into a convolutional neural network and achieves an accuracy of 95.45%. The algorithm proposed in this paper uses higher-order spectral analysis to represent the one-dimensional signal as a two-dimensional matrix as the input to the neural network, and its accuracy will be greatly improved, which is a novel method. The accuracy of the algorithm proposed in this paper, whose algorithm is high compared to that of other algorithms in the literature, reaches 99.26% accuracy in the test set. Compared with literature (J. Rajashekar & A. Yadav, 2022) and literature (A. Bhuyan, B. K. Panigrahi, K. Pal & S. Pati, 2022), the focus of this paper is on converting the time-series data into images. With the algorithms in this paper, key fault features can be extracted that can be accurately identified by the neural network. In terms of dealing with the classification of transmission line faults, this paper has some research value by converting the time-series data into images that can be used to classify faults by ResNet50.

**5. Conclusion**

This paper is the first application of higher-order spectral analysis method to transmission line fault diagnosis in deep learning, which was first proposed in the field of medical heart-lung sound detection. The fault timing signal of transmission line is transformed into a two-dimensional feature image by the higher-order spectral analysis method, i.e., the one-dimensional signal is represented as a two-dimensional matrix, and then the fault diagnosis originally applied to RNN is changed into image processing in CNN. The neural network model is constructed by Matlab, and the simulation comparison results show that the proposed method has high accuracy and practicality, and the diagnosis results are not affected by the fault distance and transition resistance.

The current technology of neural networks in image processing is very mature, and this paper converts the time-series signals into images, which is more general and more consistent with the mechanism of most problems compared to RNN. Deep learning has been very widely used in computer vision, and visual image data is two-dimensional data, while data in the field of transmission line fault diagnosis, which comes from sensor acquisition, is a typical one-dimensional time series. If time series or one-dimensional arrays are transformed into images, and then deep learning models are applied to do analysis, it is a very good method.

## References

- A. Bhuyan, B. K. Panigrahi, K. Pal and S. Pati, (2022). "Convolutional Neural Network Based Fault Detection for Transmission Line," 2022 International Conference on Intelligent Controller and Computing for Smart Power (ICICCSP), Hyderabad, India, pp. 1-4.
- J. Rajashekar and A. Yadav, (2022). "Transmission lines Fault Detection and Classification Using Deep Learning Neural Network," 2022 Second International Conference on Advances in Electrical, Computing, Communication and Sustainable Technologies (ICAECT), pp. 1-6.
- L. Gagliano, E. B. Assi, M. Sawan and D. K. Nguyen, (2018). Bicoherence of Intracranial EEG: A Novel Precursor of Seizure Activity in Canine Epilepsy, *2018 IEEE Life Sciences Conference (LSC)*, pp. 93-96.
- Li LF, Rao D, Fan R, Zhang H, Wang J, Luo HY, Liu Z, Xu GH, (2022). A transmission line fault discrimination method based on bidirectional LSTM and attention mechanism. *Guangdong Electric Power*, 35(11), 91-98.
- Liu F, Li YK, Gao F, et al, (2021). Transmission line fault diagnosis based on wavelet scattering cooperative BiLSTM. *Foreign Electronic Measurement Technology*, 40(12), 165-172. DOI:10.19652/j.cnki.femt.2103180.
- M. Li, Y. Yu, T. Ji and Q. Wu, (2019). "On-line Transmission Line Fault Classification using Long Short-Term Memory," 2019 IEEE 12th International Symposium on Diagnostics for Electrical Machines, Power Electronics and Drives (SDEMPED), pp. 513-518.
- M. R. Bishal, S. Ahmed, N. M. Molla, K. M. Mamun, A. Rahman and M. A. A. Hysam, (2021). "ANN Based Fault Detection & Classification in Power System Transmission line," 2021 International Conference on Science & Contemporary Technologies (ICSCT), pp. 1-4.
- R. Resmi, V. Vanitha, E. Aravind, B. R. Sundaram, C. R. Aswin and S. Harithaa, (2019). "Detection, Classification and Zone Location of Fault in Transmission Line using Artificial Neural Network," 2019 IEEE International Conference on Electrical, Computer and Communication Technologies (ICECCT), pp. 1-5.
- X. Liu, X. Miao, H. Jiang and J. Chen, (2021). "Box-Point Detector: A Diagnosis Method for Insulator Faults in Power Lines Using Aerial Images and Convolutional Neural Networks," in *IEEE Transactions on Power Delivery*, 36(6), pp. 3765-3773.
- X. Zhang et al, (2021). "InsuDet: A Fault Detection Method for Insulators of Overhead Transmission Lines Using Convolutional Neural Networks," in *IEEE Transactions on Instrumentation and Measurement*, 70, pp. 1-12, Art no. 5018512, doi: 10.1109/TIM.2021.3120796.
- Y. Bao and T. Chen, (2020). "Automatic Identification and Defect Diagnosis of Transmission Line Insulators Based on YOLOv3 Network," 2020 International Conference on Communications, Information System and Computer Engineering (CISCE), pp. 372-375.
- Yu F, Zhao J, Qiu Z. Y et al, (2022). Deep learning-based diagnosis model for chronic obstructive pulmonary disease. *Chinese Journal of Biomedical Engineering*, 41(05), 558-566.
- Z. Wan, L. Hui and L. Yongkang, (2020). "Research on Fault Diagnosis of Transmission Lines based on VMD and Bidirectional LSTM," 2020 7th International Forum on Electrical Engineering and Automation (IFEEA), pp. 445-450.

## Copyrights

Copyright for this article is retained by the author(s), with first publication rights granted to the journal.

This is an open-access article distributed under the terms and conditions of the Creative Commons Attribution license (<http://creativecommons.org/licenses/by/4.0/>).